Self-assembly

self-assembly

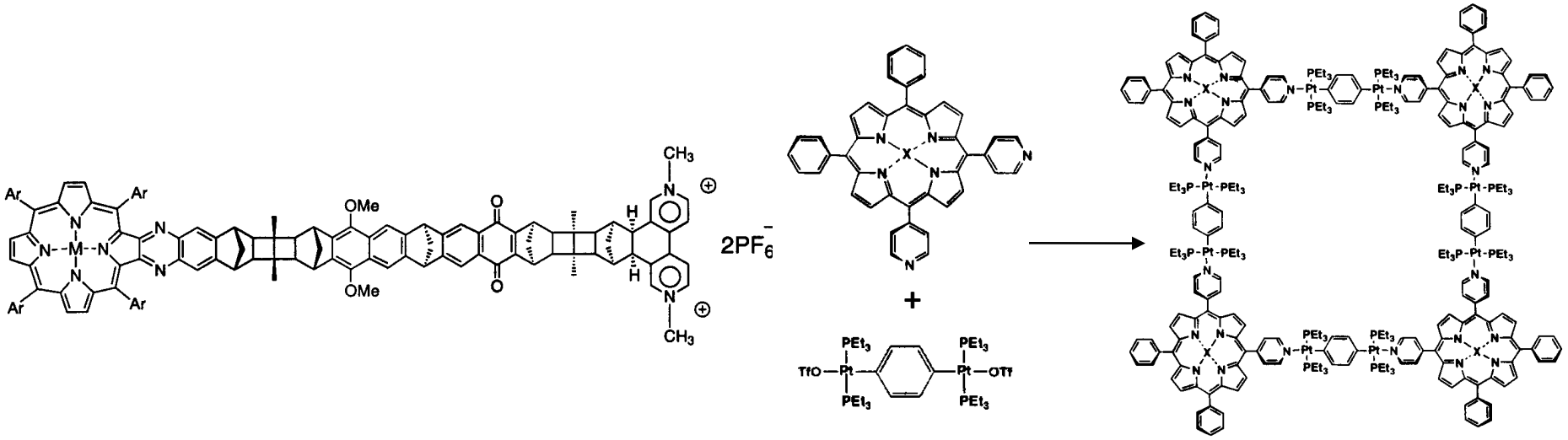

Paddon-Row *et al.*
Chem.Eur.J. **1999**, *5*, 2518

Stang *et al.*
JACS **1999**, *121*, 2741

Characteristics

building block	atom	molecule
target	molecules	assemblies
bond type	covalent	ionic, hydrophobic, metal-coordination, H-bond
bond energy	35-135 kcal/mol	2 - 20 kcal/mol
kinetic stability	high	low (dynamic structures !!!)

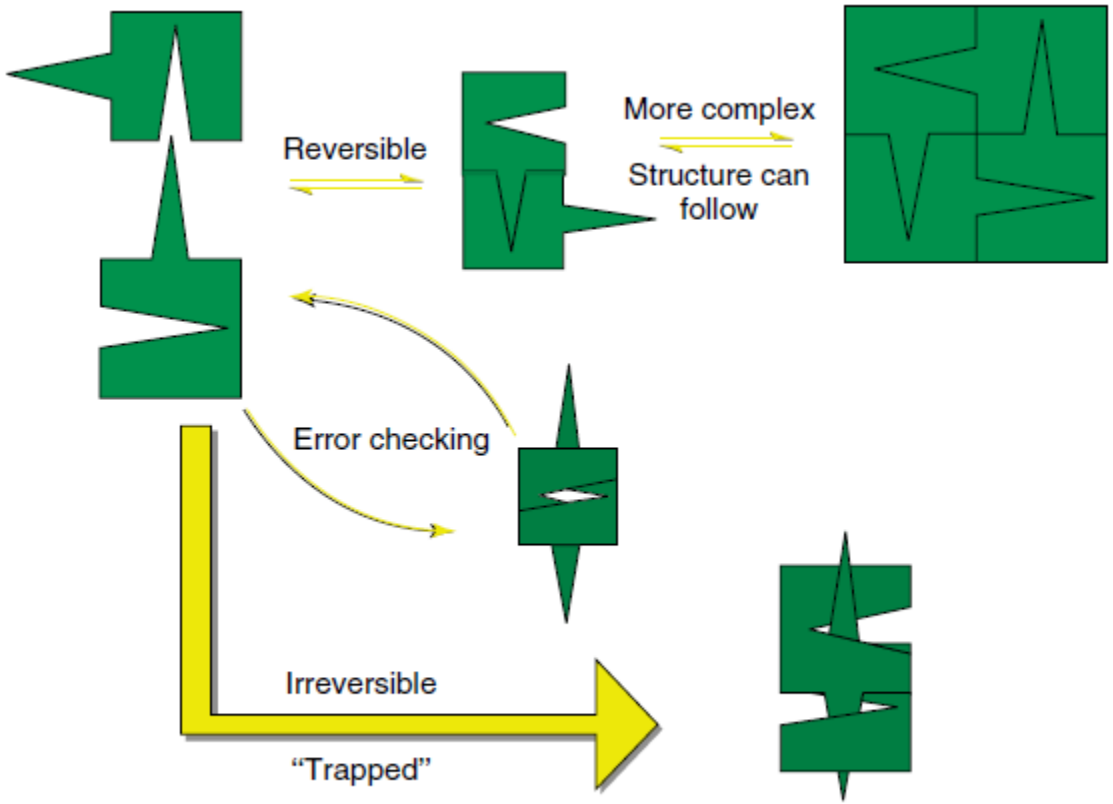

Figure 3 Comparison of reversible and irreversible steps and their effects on the supramolecular assembly.

design principles

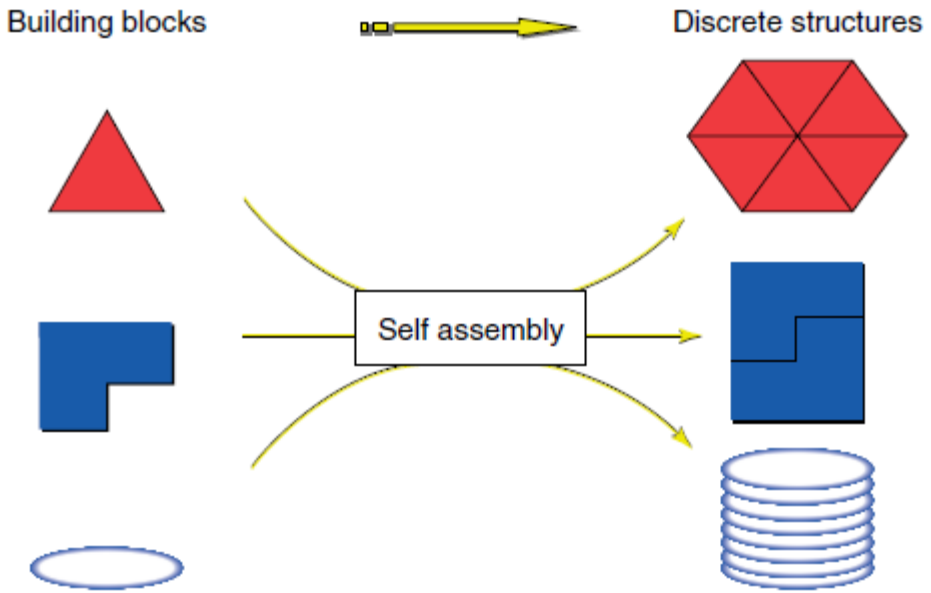

Figure 2 Schematic assembly of building blocks with various shapes to form discrete supramolecular structures.

information inserted in the building blocks

CHEMICAL REVIEWS

REVIEW

pubs.acs.org/CR

Supramolecular Coordination: Self-Assembly of Finite Two- and Three-Dimensional Ensembles

Rajesh Chakrabarty,*[,†] Partha Sarathi Mukherjee,*[,‡] and Peter J. Stang*[,†]

[†]Department of Chemistry, University of Utah, 315 South 1400 East, Salt Lake City, Utah 84112, United States

[‡]Department of Inorganic and Physical Chemistry, Indian Institute of Science, Bangalore 560012, India

2.1. Directional Bonding Approach

(coordination, H-bonds, dynamic covalent bonds)

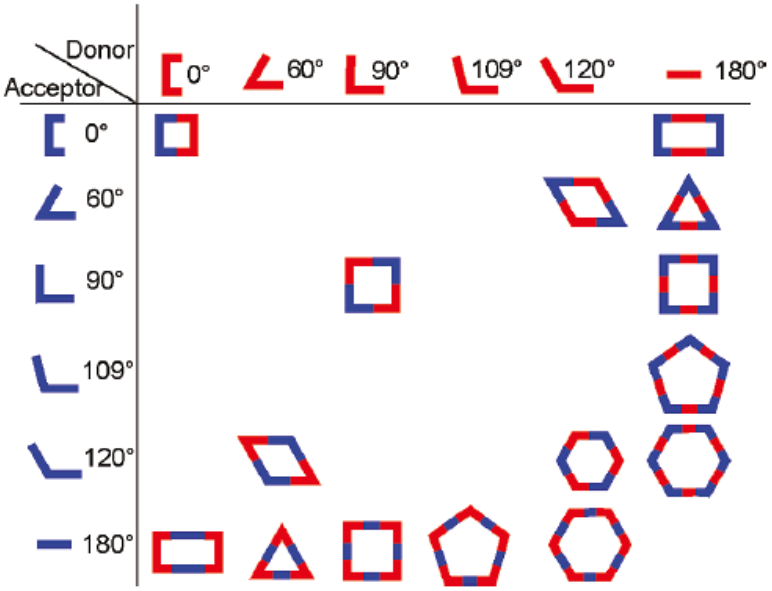

Figure 1. Combination of various building units for accessing convex polygons and canonical polyhedra.

There are two basic structural requirements for the construction of supramolecular architectures by this approach. First, the complementary precursor units must be structurally rigid with predefined bite angles; and second, the appropriate stoichiometric ratio of the precursors must be used. The donor building blocks are generally organic ligands having two or more binding sites possessing angular orientations ranging from 0 to 180° (Figure 1).

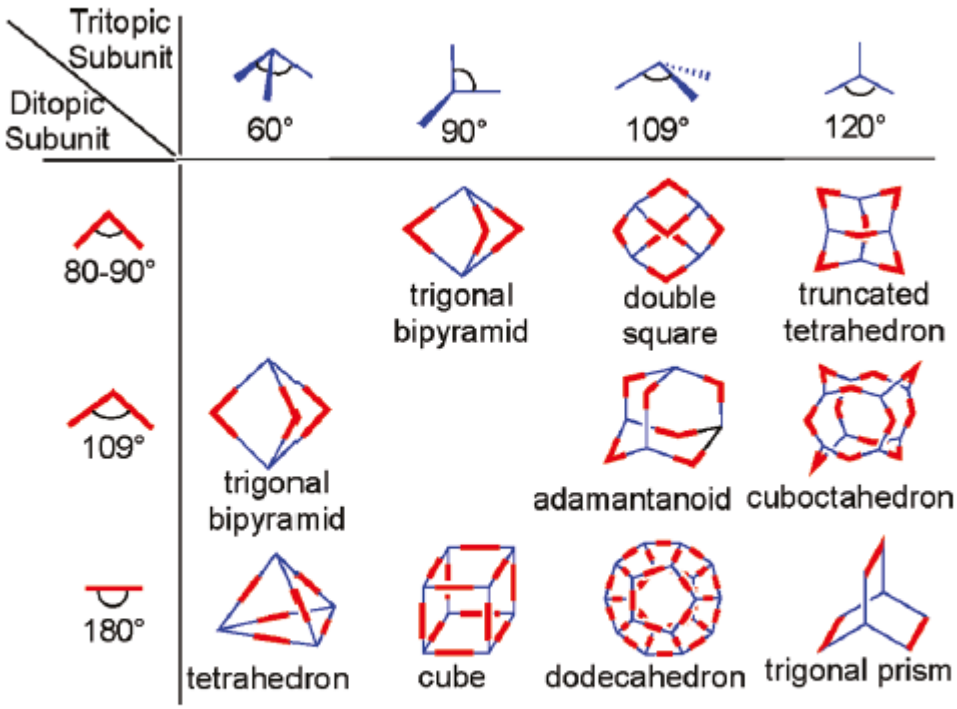

Figure 2. Three-dimensional architectures formed by the combination of ditopic and tritopic subunits by the directional bonding approach.

Preparation of a Macrocyclic Polynuclear Complex, $[(en)Pd(4,4'\text{-bpy})]_4(NO_3)_8$,[1] Which Recognizes an Organic Molecule in Aqueous Media

Makoto Fujita,* Jun Yazaki, and Katsuyuki Ogura*

Department of Synthetic Chemistry
Faculty of Engineering, Chiba University
1-33 Yayoicho, Chiba 260, Japan

Received March 23, 1990

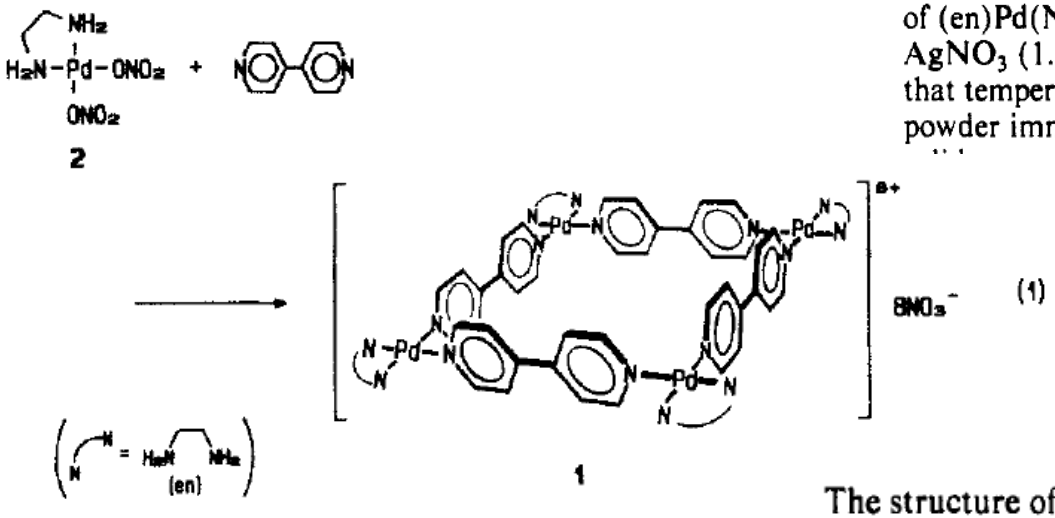

2

1

(1)

An ethanol (4 mL) solution of 4,4'-bpy (0.5 mmol) was added at room temperature to a methanol–water (1:1) solution (4 mL) of $(en)Pd(NO_3)_2$[5] (**2**), prepared from $(en)PdCl_2$[5] (0.5 mmol) and $AgNO_3$ (1.0 mmol), and the solution was stirred for 10 min at that temperature. Upon addition of ethanol (4 mL), a pale yellow powder immediately precipitated. The elemental analysis of the

The structure of this complex is estimated to be a macrocyclic tetramer **1** by the following facts: (i) all pyridine nuclei of the complex are completely equivalent in NMR spectrometry (vide ante); (ii) the empirical formula predicted by CHN analysis[6b] was reproduced even if the complex was prepared with excess 4,4'-bpy (2 equiv); (iii) right bond angles (N–Pd–N(cis) = 90°) rule out the formation of other cyclic oligomers which must have significant ring strain.[10]

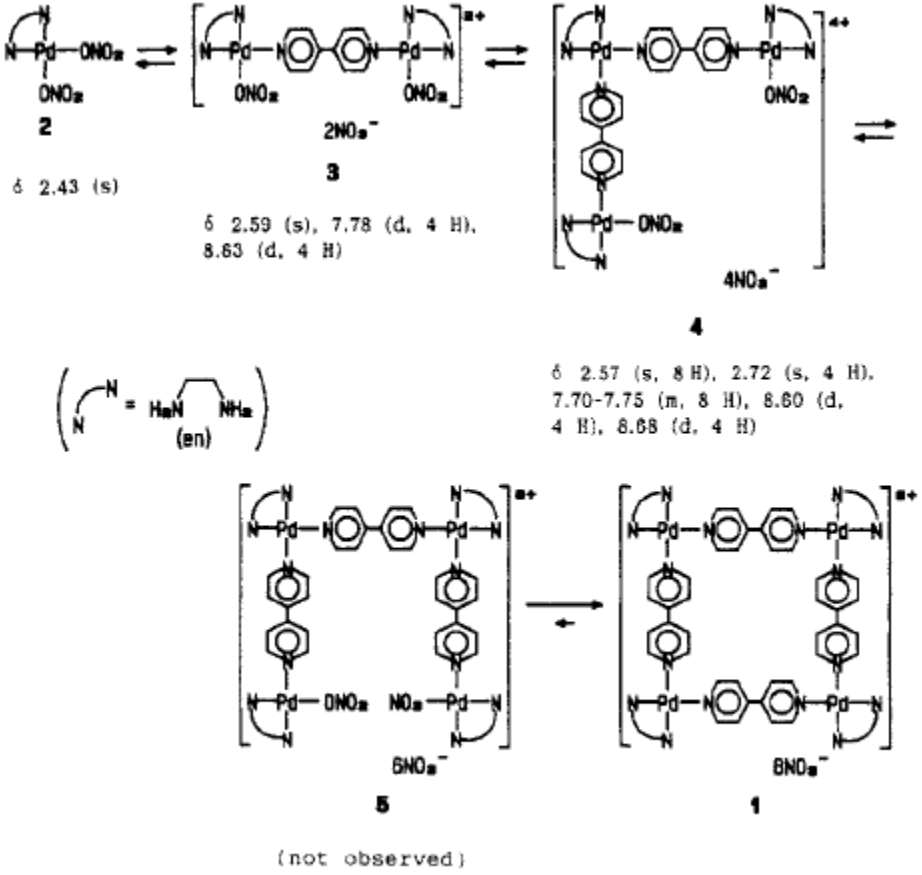

of bpy. Furthermore, the spectrum of Figure 1c (0.6 equiv of bpy) was completely identical with the spectrum obtained when pure **1** and **2** were mixed so that the ratio Pd:bpy became the same. These observations support rapid equilibrium which mainly lies on the stable cyclic tetramer **1** as shown in Scheme I. It is noteworthy that *the thermodynamic cyclization realized quantitative formation of* ***1*** without employing any special conditions such as high dilution.

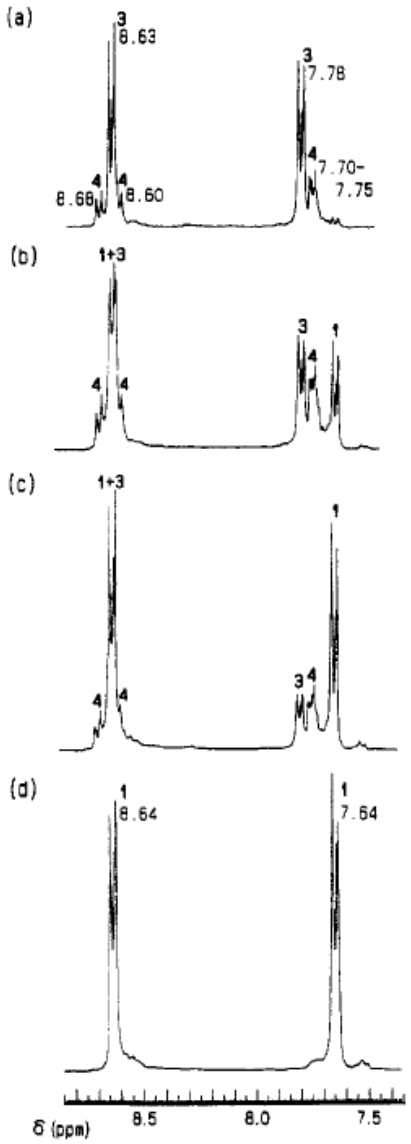

Figure 1. ^{1}H NMR spectra (270 MHz, D_2O)[8] obtained from mixtures of **2** and 4,4′-bpy: (a) **2**:bpy = 1:0.2; (b) **2**:bpy = 1:0.4; (c) **2**:bpy = 1:0.6; (d) **2**:bpy = 1:0.9.

Self-Assembled $M_{24}L_{48}$ Polyhedra and Their Sharp Structural Switch upon Subtle Ligand Variation

Qing-Fu Sun,[1] Junji Iwasa,[1] Daichi Ogawa,[1] Yoshitaka Ishido,[1] Sota Sato,[1] Tomoji Ozeki,[2] Yoshihisa Sei,[3] Kentaro Yamaguchi,[3] Makoto Fujita[1]*

Self-assembly is a powerful technique for the bottom-up construction of discrete, well-defined nanoscale structures. Large multicomponent systems (with more than 50 components) offer mechanistic insights into biological assembly but present daunting synthetic challenges. Here we report the self-assembly of giant $M_{24}L_{48}$ coordination spheres from 24 palladium ions (M) and 48 curved bridging ligands (L). The structure of this multicomponent system is highly sensitive to the geometry of the bent ligands. Even a slight change in the ligand bend angle critically switches the final structure observed across the entire ensemble of building blocks between $M_{24}L_{48}$ and $M_{12}L_{24}$ coordination spheres. The amplification of this small initial difference into an incommensurable difference in the resultant structures is a key mark of emergent behavior.

28 MAY 2010 VOL 328 **SCIENCE** www.sciencemag.org

see PDF

2.2. Symmetry Interaction Approach

clusters using metal−ligand bonds. It is based on the geometric relationship between the chelating ligands and the metals used. The strong binding affinity and coordination mode of chelating ligands, along with the inherent symmetry of the coordination sites available on the naked metal center, act as the driving force for the assembly process. In general, multibranched chelating ligands with rigid backbones are used in conjunction with transition metals or main group metals. The orientation of the multiple binding sites that are rigidly fixed is critical to the selectivity of a particular molecular geometry and helps to avoid the formation of oligomers and polymers. Similar to the directional bonding approach, it relies on the thermodynamic control and kinetic reversibility for error checking and self-correction.

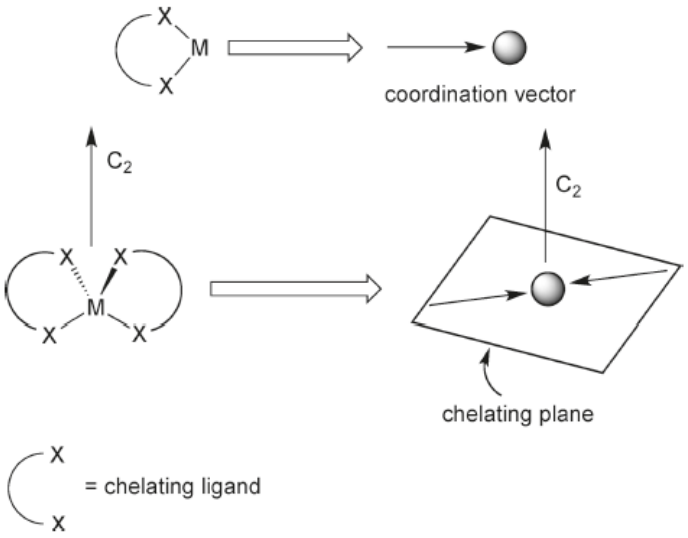

Figure 3. Coordinate vector and chelate plane for the symmetry interaction method.

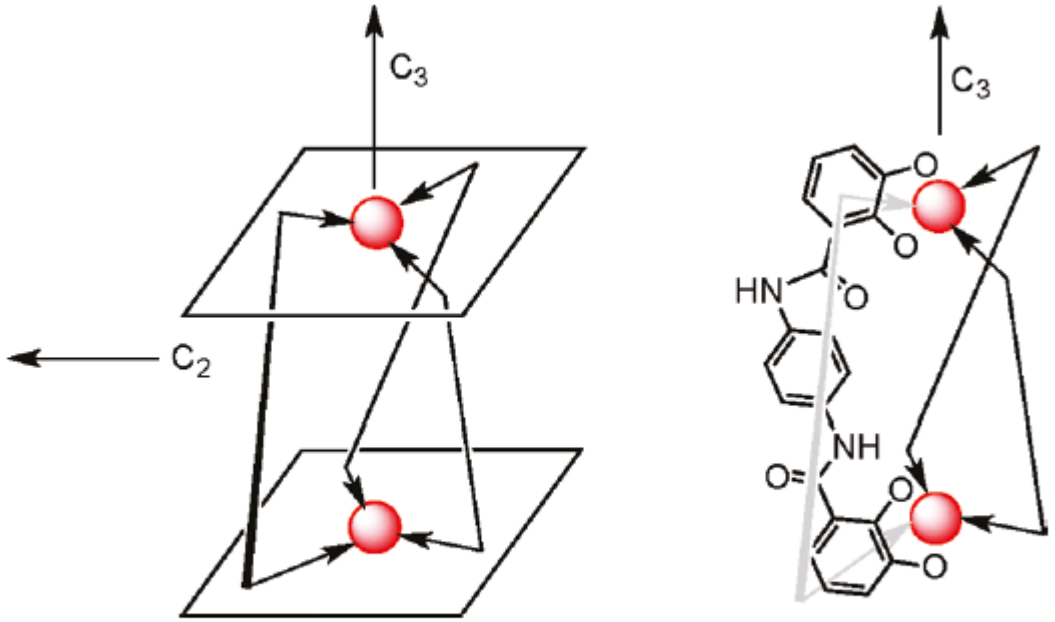

Figure 4. Design of a D_3-symmetrical triple helicate.

For example, to design a M_2L_3 triple helicate having an idealized D_{3h} symmetry, it must be ensured that both the C_2 and C_3 axes are orthogonal and are preprogrammed into the chelating ligand and the metal center. Since the two pseudo-octahedral metal centers share the same C_3 axis, the two chelating planes must be parallel to achieve the triple helicate (Figure 4).

2.3. Paneling Approach

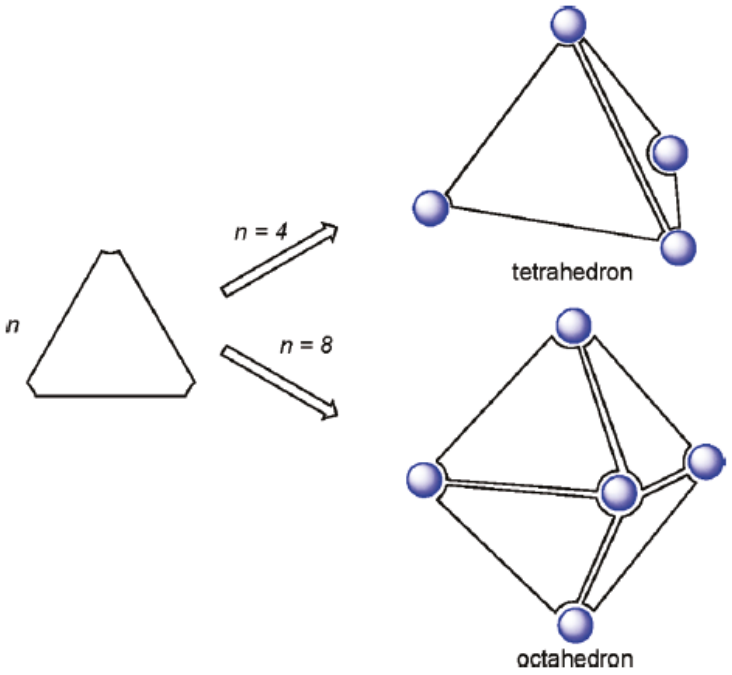

Figure 6. Representation for assembling a tetrahedron and an octahedron using triangular panels.

equilateral triangles, squares, and pentagons.[10] Thus, 3D molecular architectures can, in principle, be designed by reducing these polyhedra to molecular components. For example, a tetrahedron can be designed by stitching together four triangular panels, while an octahedron can be prepared by bringing together eight such triangular panels (Figure 6). Similarly, the paneling of squares

Self-assembly of ten molecules into nanometre-sized organic host frameworks

Makoto Fujita*, Daichi Oguro*, Mayumi Miyazawa*, Hiroko Oka*, Kentaro Yamaguchi† & Katsuyuki Ogura*

* Department of Applied Chemistry, Faculty of Engineering and
† Chemical Analysis Center, Chiba University, Yayoicho, Inageku, Chiba 263, Japan

a

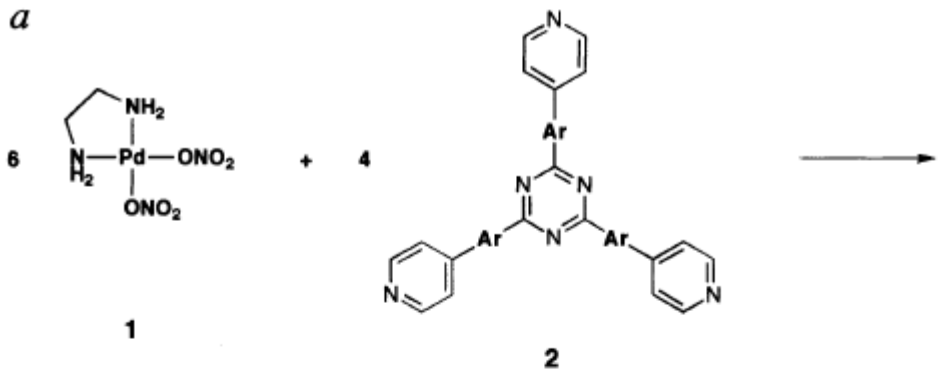

b

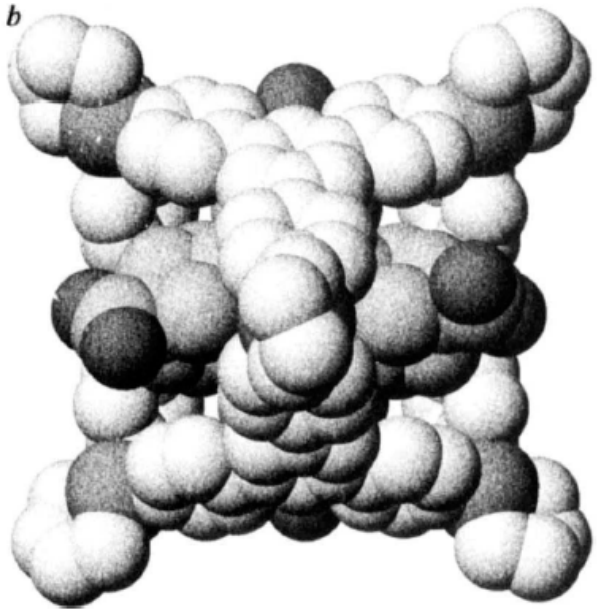

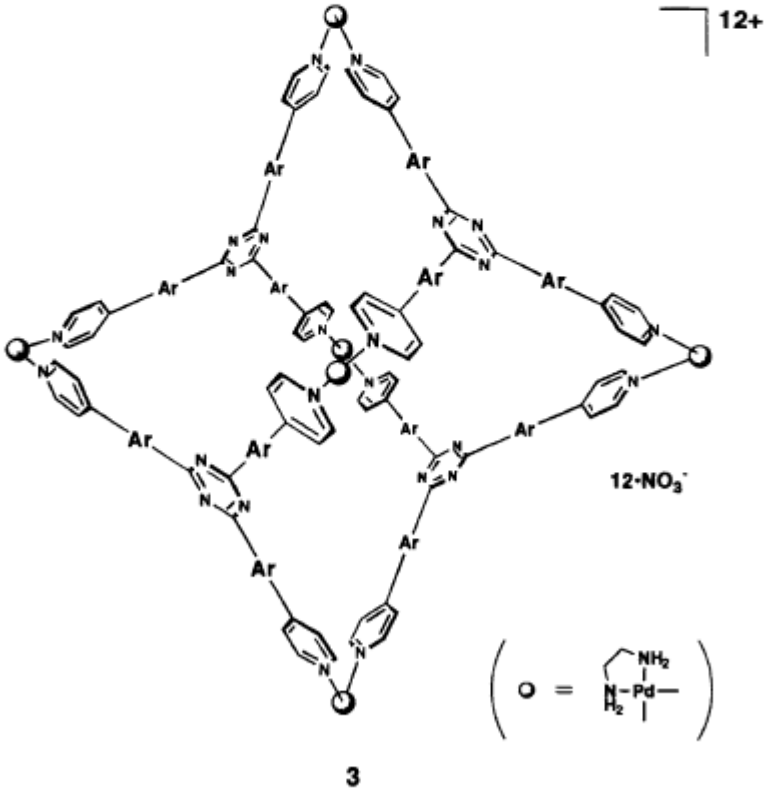

FIG. 1 *a*, The reaction scheme for the self-assembly of compound **3**. *b*, The crystal structure of the clathrate complex **3a′**·(**4**)$_4$ (a space-filling model presentation). A crystal with dimensions 0.42 × 0.40 × 0.34 mm

a: Ar = none; **b**: Ar = 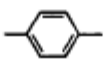 ; **c**: Ar = 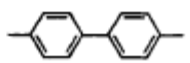

The structure of **3a** was confirmed by X-ray crystallographic analysis of its clathrate complex with four adamanyl carboxylate ions (**4**) (Fig. 1*b*). Crystals were grown by allowing an aqueous

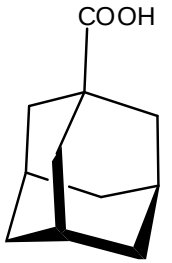

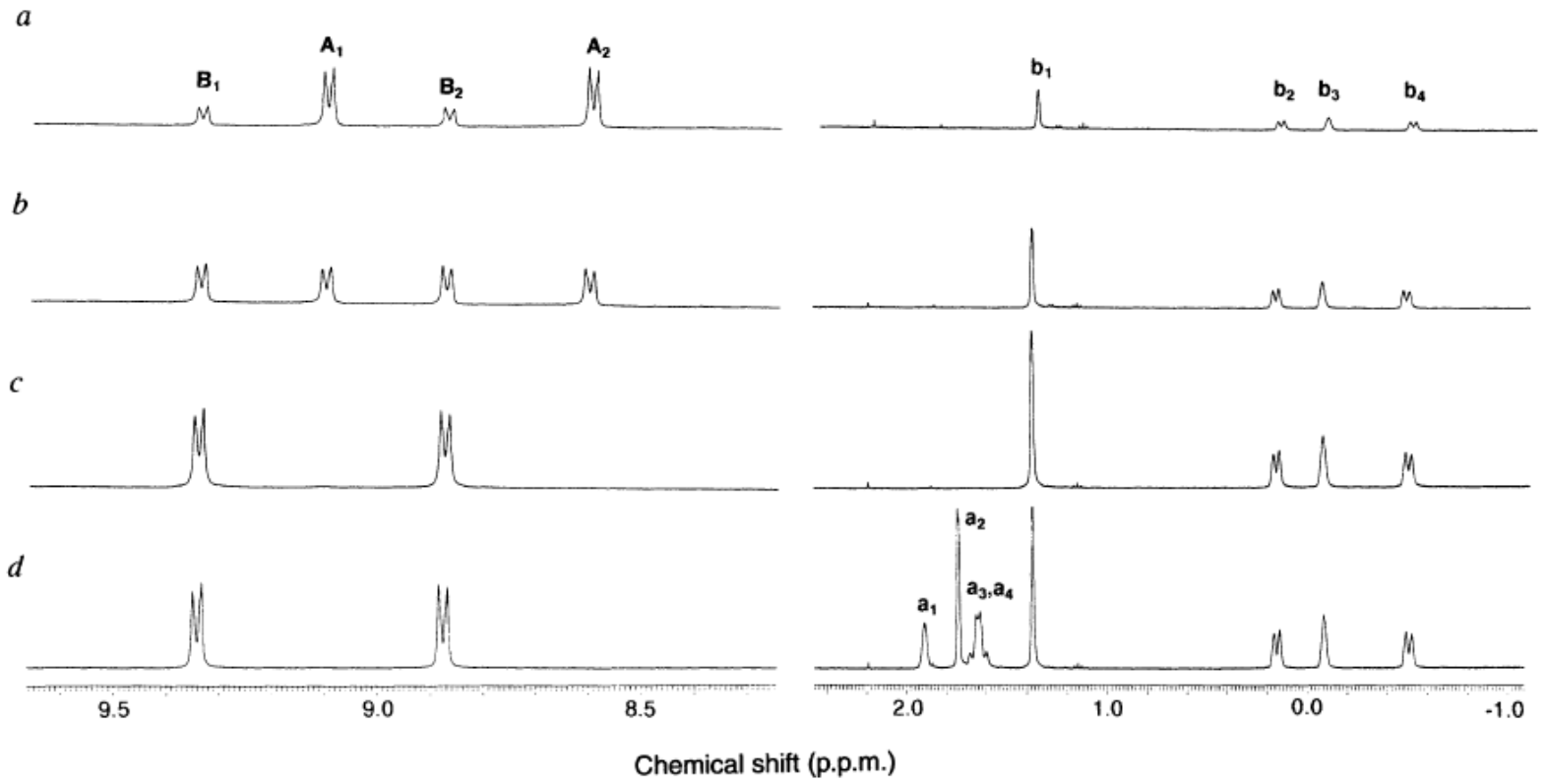

FIG. 3 Monitoring of the titration of **3a** with **4** by ^{1}H NMR (400 MHz, D_2O, external TMS). The ratios **3a**:**4** are: *a*, 1:1; *b*, 1:2; *c*, 1:4; *d*, 1:8. Components (signals) are as follows: uncomplexed **3a** (peaks A_1 and A_2); complexed **3a** (peaks B_1 and B_2); uncomplexed **4** (peaks a_1, a_2, a_3 and a_4); complexed **4** (peaks b_1, b_2, b_3 and b_4).

2.4. Weak Link Approach

Scheme 1

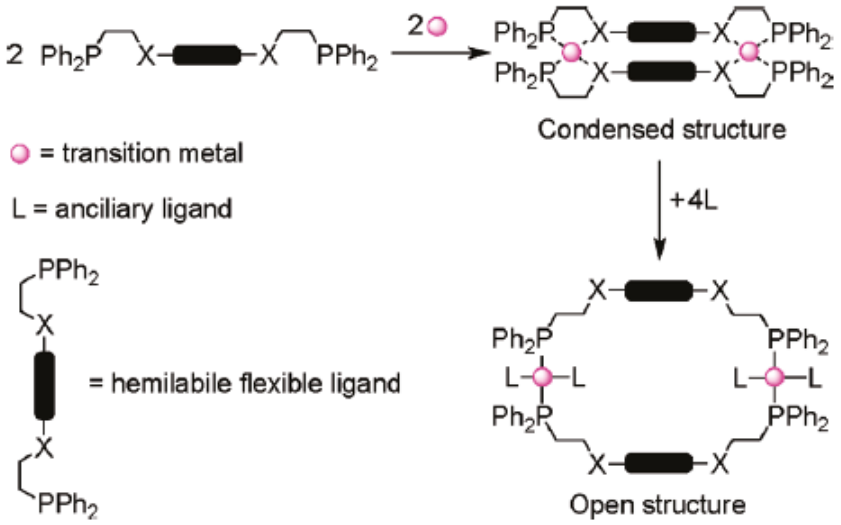

In this design strategy, pioneered by Mirkin and co-workers, both 2D and 3D supramolecular assemblies are accessible using hemilabile ligands and transition metals.[11] The hemilabile, flexible ligands coordinate in a bidentate chelating mode to the metal center such that one of the metal−ligand bonds is weaker than the other. The formation of the kinetically controlled product is driven by the chelating effect of the bidentate ligands and the $\pi-\pi$ interaction between the two central bridging units (Scheme 1). The weak ligands of this condensed intermediate structure can be selectively displaced upon treatment with small molecules or ions that have stronger affinity for the metal center, thereby generating the thermodynamically controlled product.

see PDF

What about hydrogen bonding ?

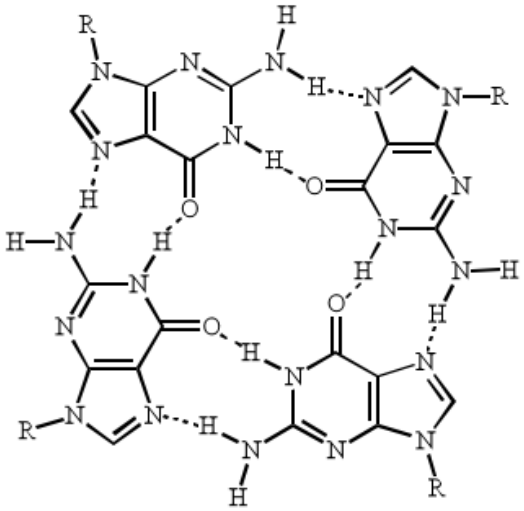

G-quartet

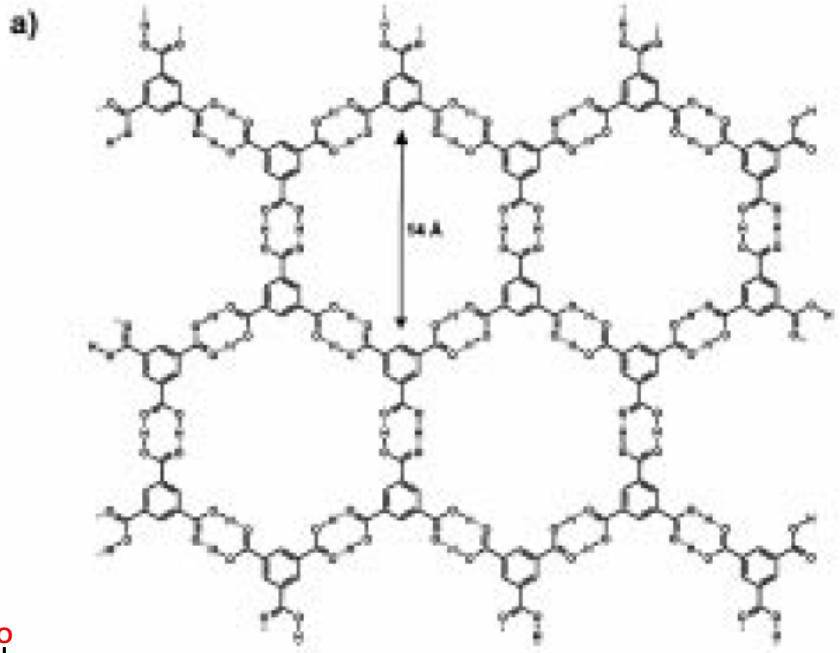

trimesic acid

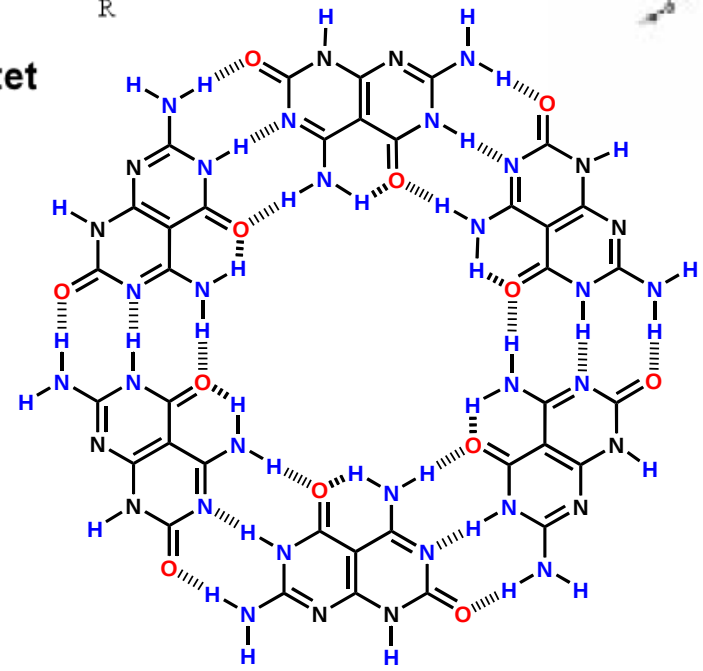

rosette

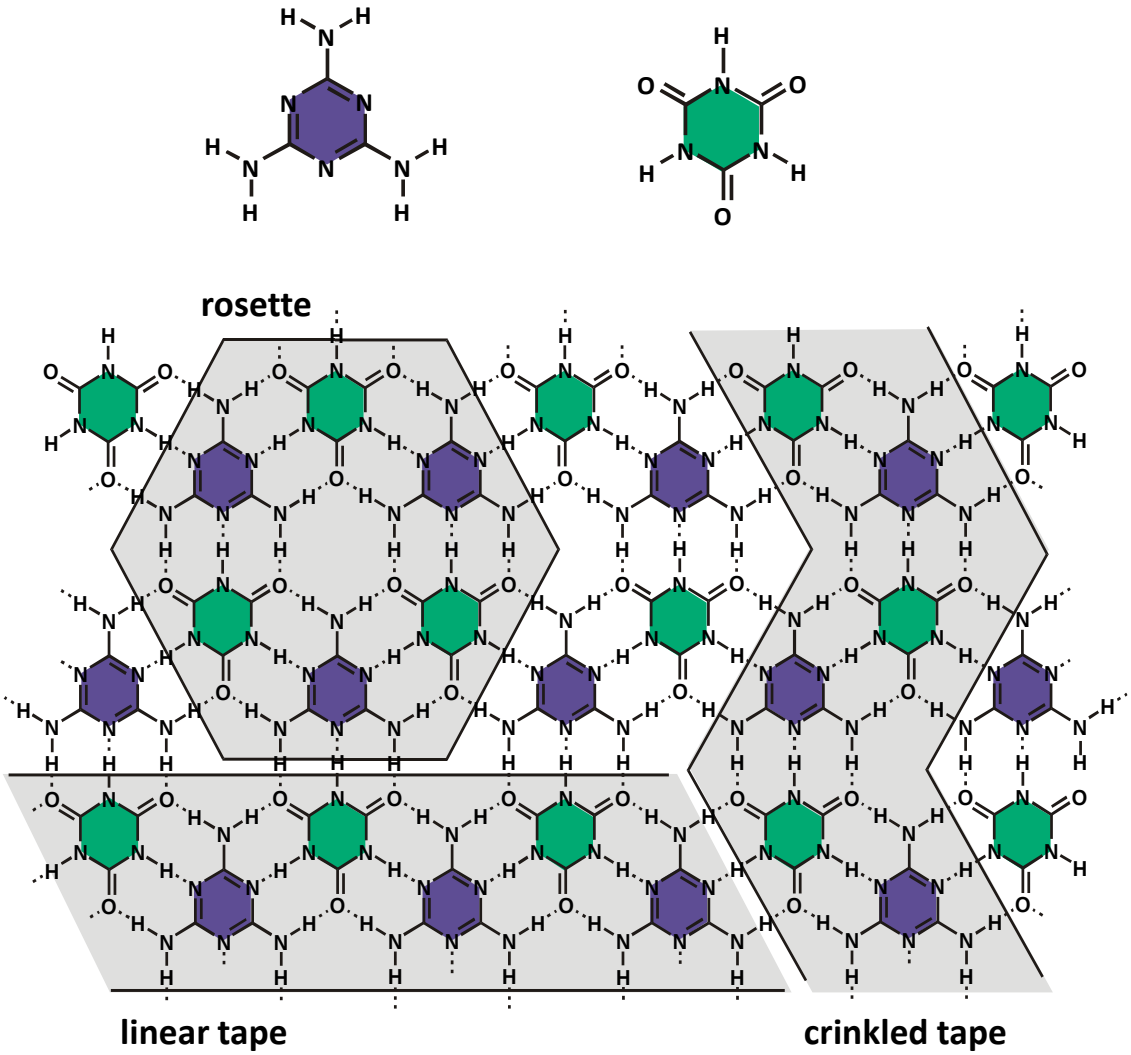
rosette
linear tape
crinkled tape

Isolation of the rosette motif

- peripheral crowding

Scheme 1

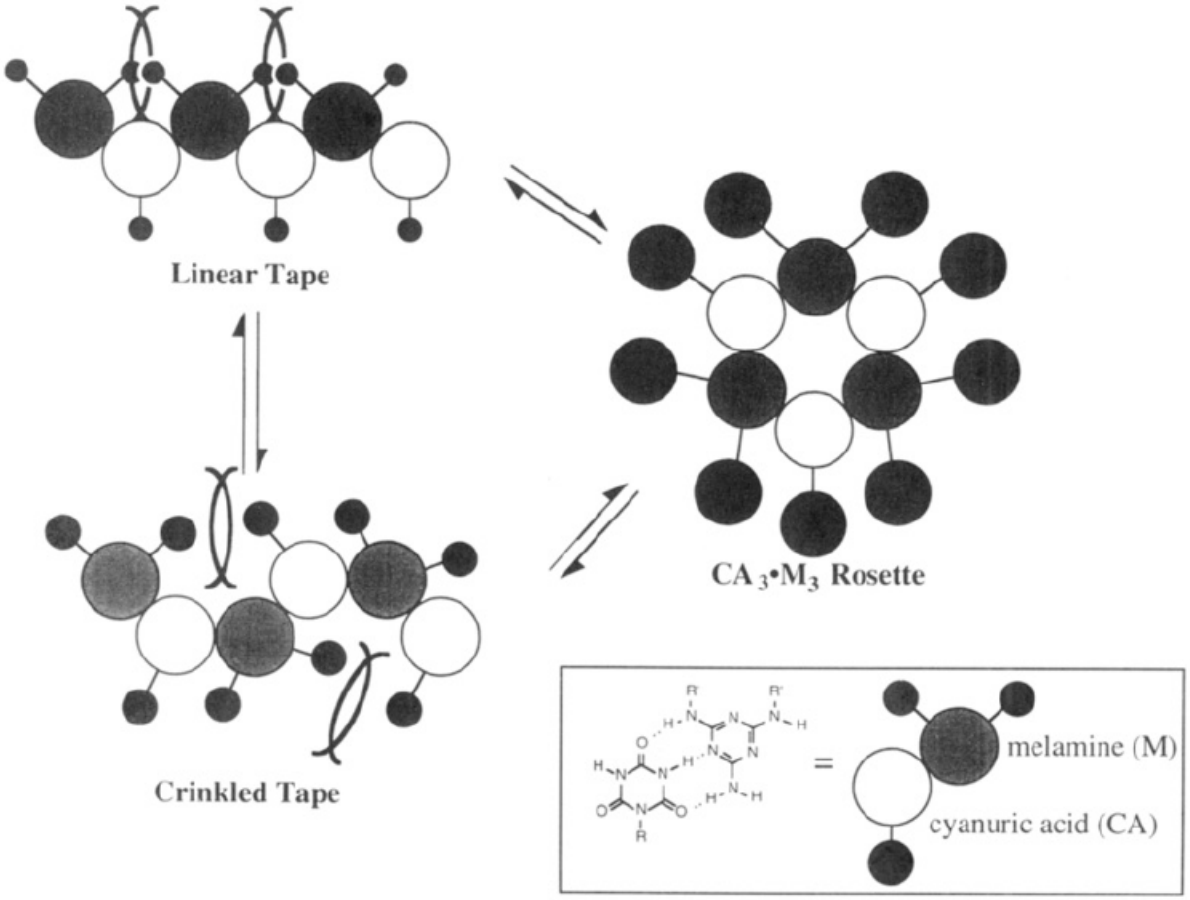

Whitesides

Acc. Chem. Res. **1995,** *28,* 37−44

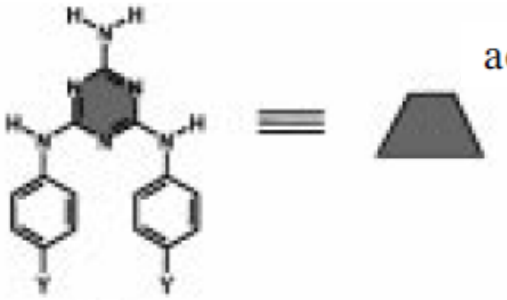

18

Y = F, Cl, CH_3, $C(=O)OCH_3$, $C(CH_3)_3$

acid (BAR) (Scheme 12).[162, 163] Linear tapes are formed preferentially with melamines with small substituents Y, such as F, Cl, or CH_3. Increasing the size of substituent Y, for example, $C(=O)OCH_3$, promotes the selective formation of crinkled tapes, primarily as a result of the relief of unfavorable steric interactions between the Y substituents on adjacent melamine units that are present in the corresponding linear tapes. A further increase in size, for example, when Y is $C(CH_3)_3$, finally gives exclusively the rosette structure, in which all the repulsive steric interactions are minimized relative to those in the corresponding tapelike structures.

Isolation of the rosette motif

- covalent preorganization

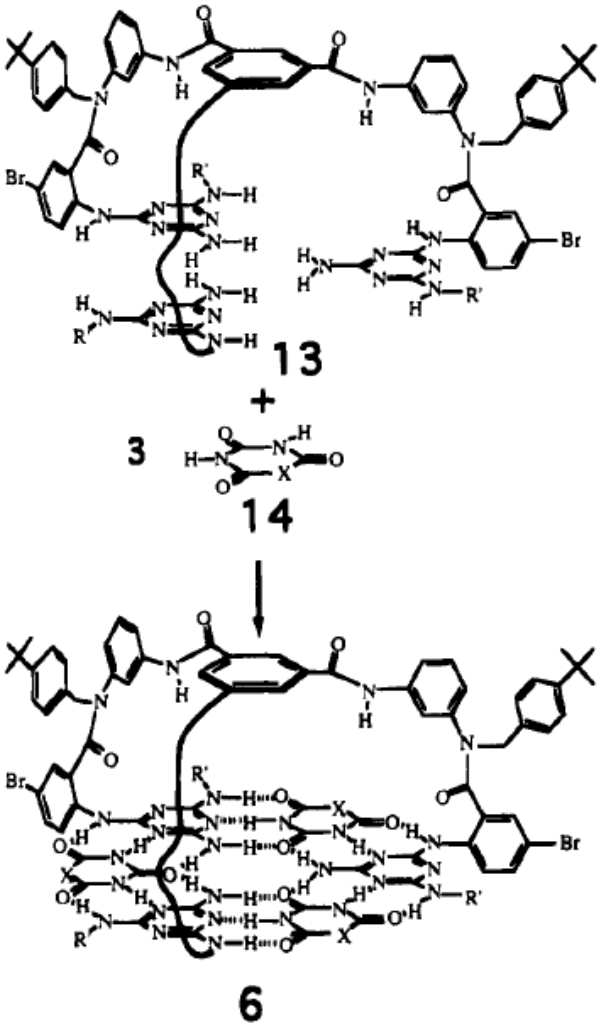

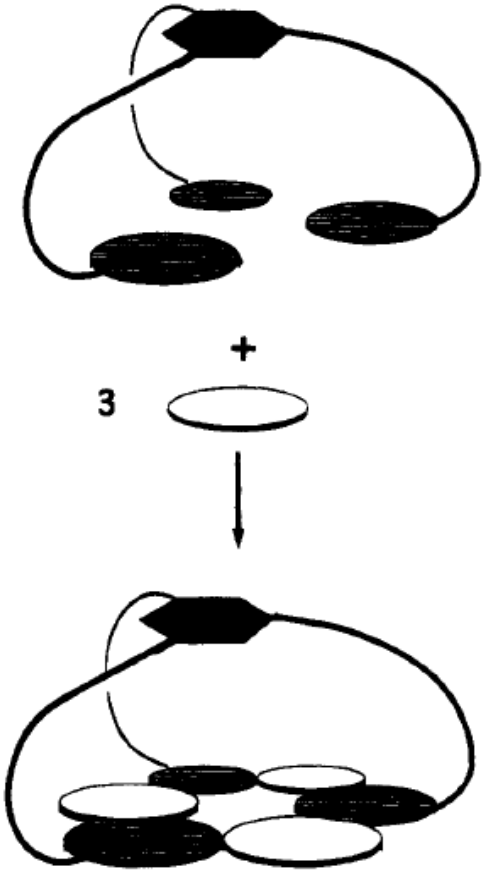

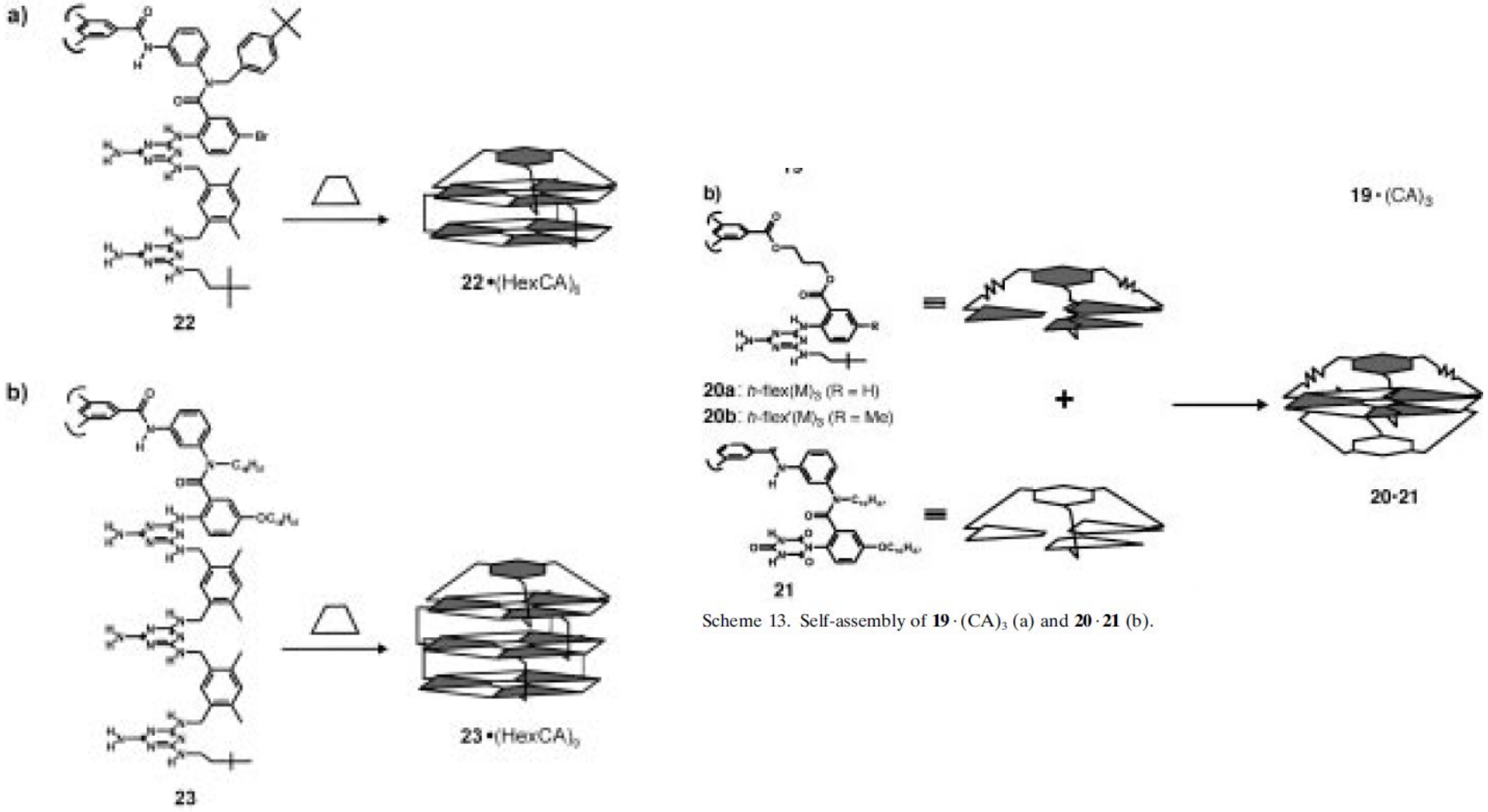

Scheme 13. Self-assembly of **19** · $(CA)_3$ (a) and **20** · **21** (b).

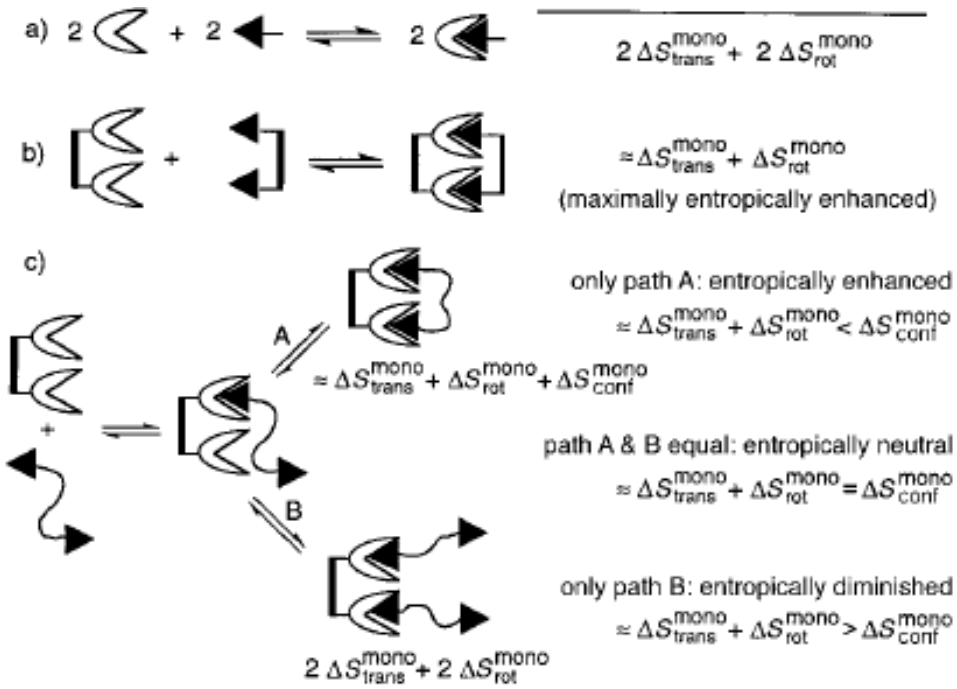

Entropy

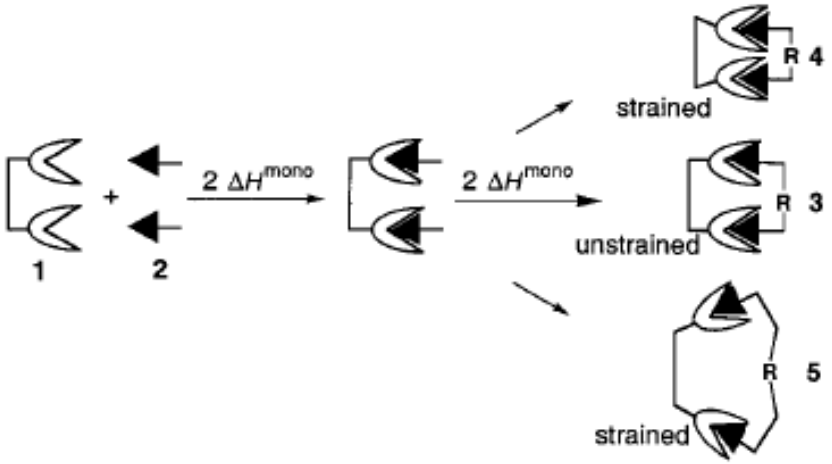

Enthalpy

Positive cooperativity is due to entropic and enthalpic contributions to binding.

Entropy: loss of motion of the molecule, including internal rotation and vibrations (contribution already paid for in connecting together the recognition elements)

Enthalpy: secondary functional groups interactions, conformational changes, polarization of the interacting groups

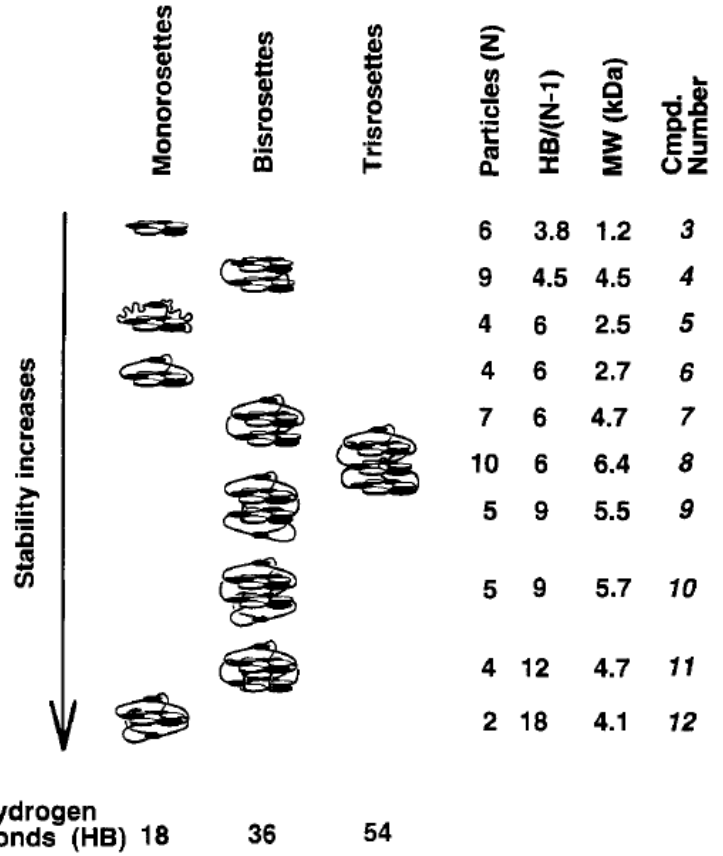

Figure 3. Structures based on the CA·M lattice, arranged in approximate order of stability. These structures are also organized by the number of rosettes (designated mono-, bis-, and tris-) they incorporate. Only one conformational isomer of each aggregate is shown; the stable conformer is, in general, not known. "Particles" is the number (N) of separate molecules comprising the aggregates—the larger the value, the greater the unfavorable entropic cost of aggregation. HB is the number of hydrogen bonds in the aggregates—the larger the value, the greater the favorable enthalpic gain of aggregation. HB/(N − 1) is an empirical parameter incorporating these trends; it is discussed in more detail in the text. MW is molecular weight of the aggregate. Aggregates discussed in the text are identified by compared number, (Cmpd. Number).

What about 3D-hydrogen bonded structures ?

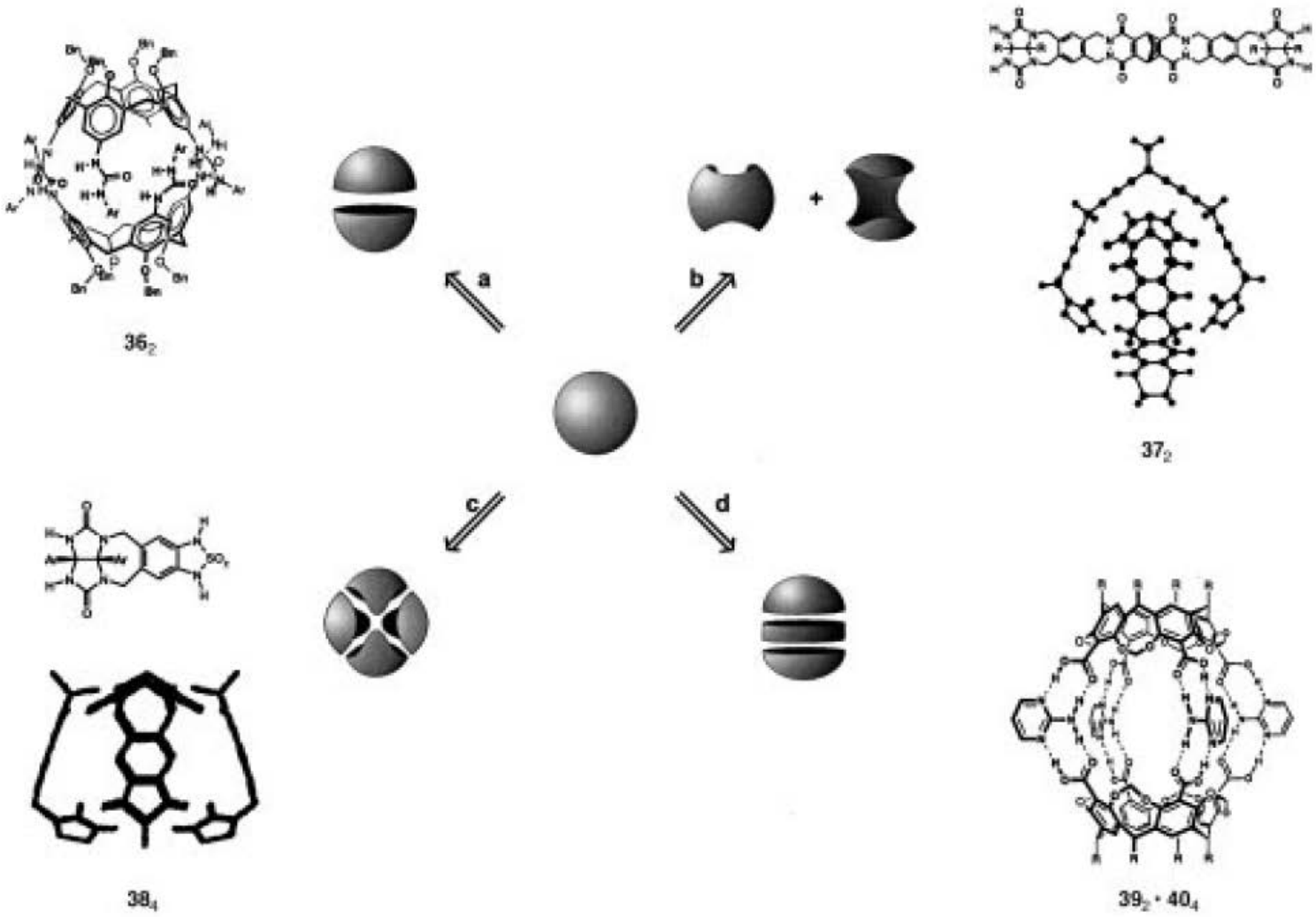

Scheme 23. Four strategies for the noncovalent synthesis of molecular containers.

How reliable is the self-assembly process ?

J|A|C|S
ARTICLES
Published on Web 03/27/2003

Self-Sorting: The Exception or the Rule?

Anxin Wu and Lyle Isaacs*

Contribution from the Department of Chemistry and Biochemistry, University of Maryland, College Park, Maryland 20742

Received October 11, 2002; E-mail: LI8@umail.umd.edu.

Abstract: In this paper, we pose the question of whether self-sorting in designed systems is exceptional behavior or whether it is likely to become a more general phenomenon governing molecular recognition and self-assembly. To address this question we prepared a mixture comprising two of Davis' self-assembled ionophores, Rebek's tennis ball and calixarene tetraurea capsule, Meijer's ureidopyrimidinone, Reinhoudt's calixarene bis(rosette), and two molecular clips in $CDCl_3$ solution and observed the behavior of this ensemble by ^1H NMR. As hypothesized, high-fidelity self-sorting behavior was observed. The influence of several key variables—temperature, concentration, equilibrium constants, and the presence of competitors—on the fidelity of self-sorting is described. These results show that self-sorting is neither the exception nor the rule. They suggest, however, that the subset of known molecular aggregates that exceed the criteria required for thermodynamic self-sorting is larger than previously appreciated and potentially quite broad.

see PDF

DNA Nanofabrication

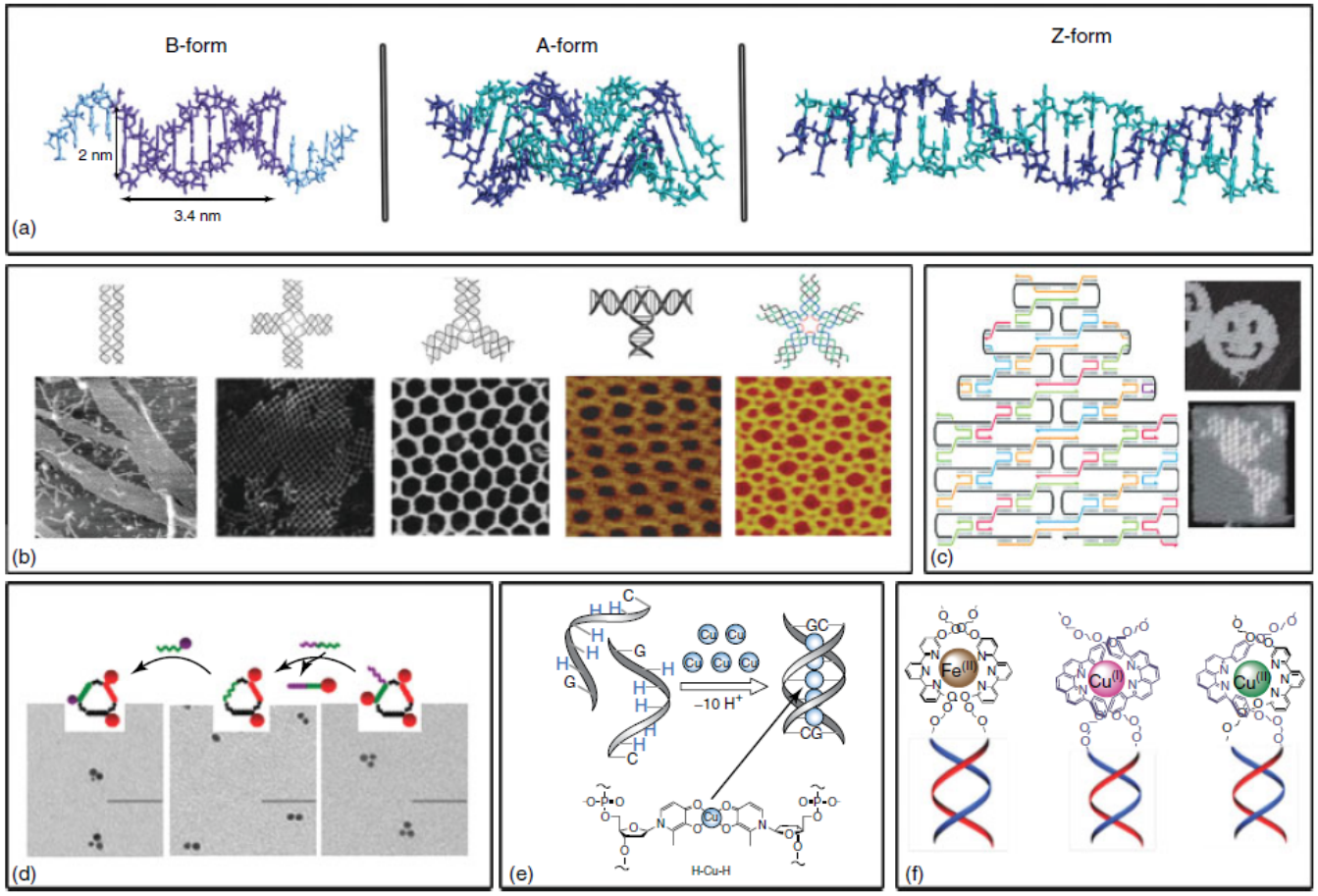

Figure 1 DNA structure and examples of DNA assembly: (a) right-handed B- and A-forms and left-handed Z-form of DNA duplexes and (b) DNA tiles, assembled from (i) double crossover (DX), (ii) cross-motif (CM), (iii) 3-point star, (iv) T-junction, and (v) 5-point star into periodic 2D arrays. (c) DNA origami. (d) Geometrically well-defined ssDNA templates with organic vertices are used to organize gold nanoparticles and encoded to allow for write/erase experiments. (e) Hydroxypyridone insertions into DNA are used to selectively coordinate Cu(II) within the DNA duplex. (f) Two different ligands are site specifically incorporated to generate DNA-templated coordination environments selective for metals.

DNA Nanofabrication

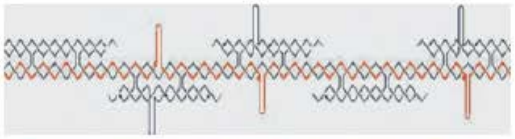

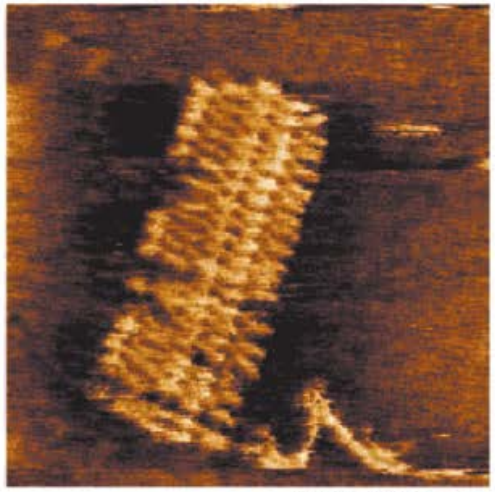

250x250nm

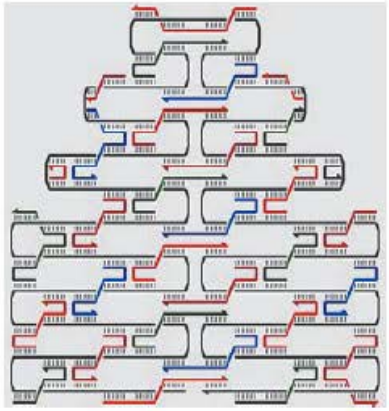

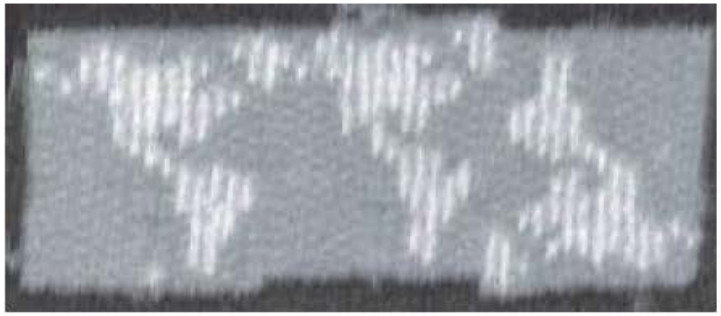

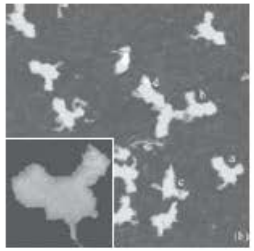

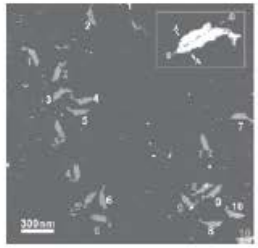

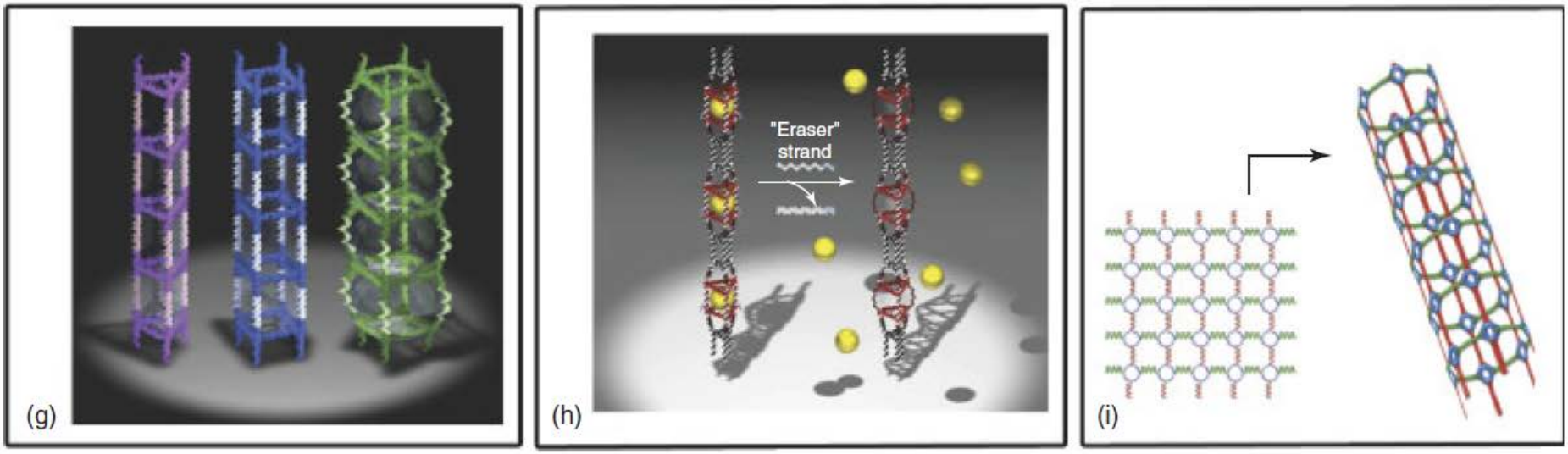
(g)
"Eraser"
strand
(h)
(i)

Self-assembly beyond noncovalent interactions

Table 1 Reversible covalent reactions.

C=N exchange

Transmination	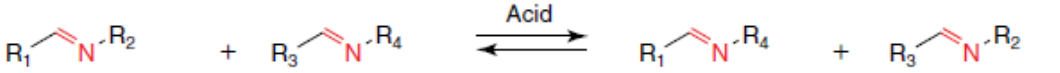	Acid	
Hydrazone exchange	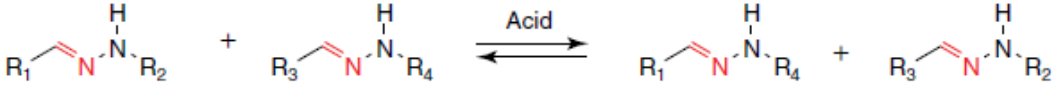	Acid	
Oxime exchange	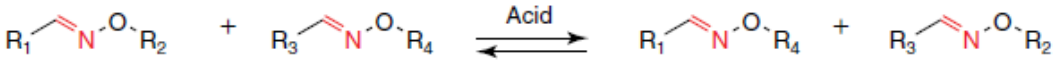	Acid	

Acyl exchange

Transesterification	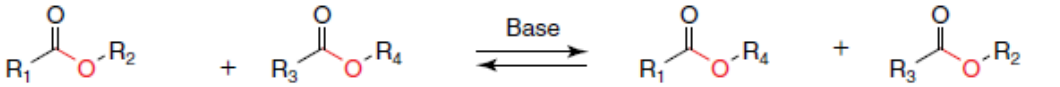	Base	
Transthioesterification	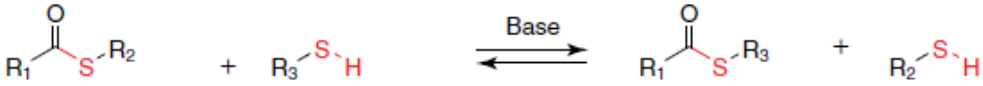	Base	
Transamidation	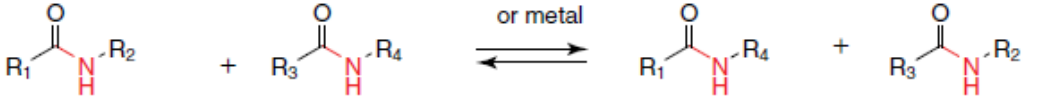	Protease or metal	
Michael-addition	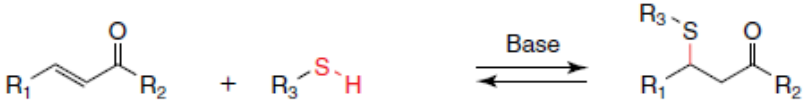	Base	

Miscellaneous

Disulfide exchange	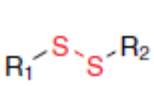	+	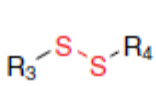	R-S	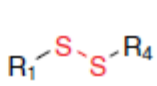	+	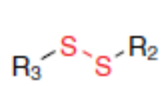
Boronic ester exchange	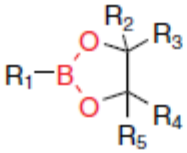	+	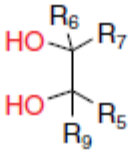	Base	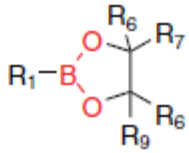	+	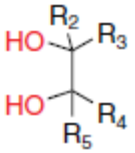
Olefin metathesis	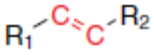	+	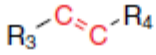	Grubbs catalyst	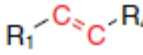	+	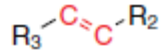
Acetal exchange	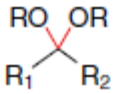	+	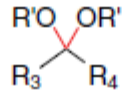	Acid	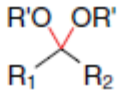	+	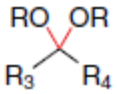
Diels–Alder	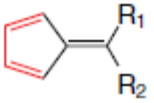	+	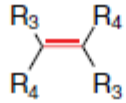		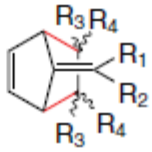		

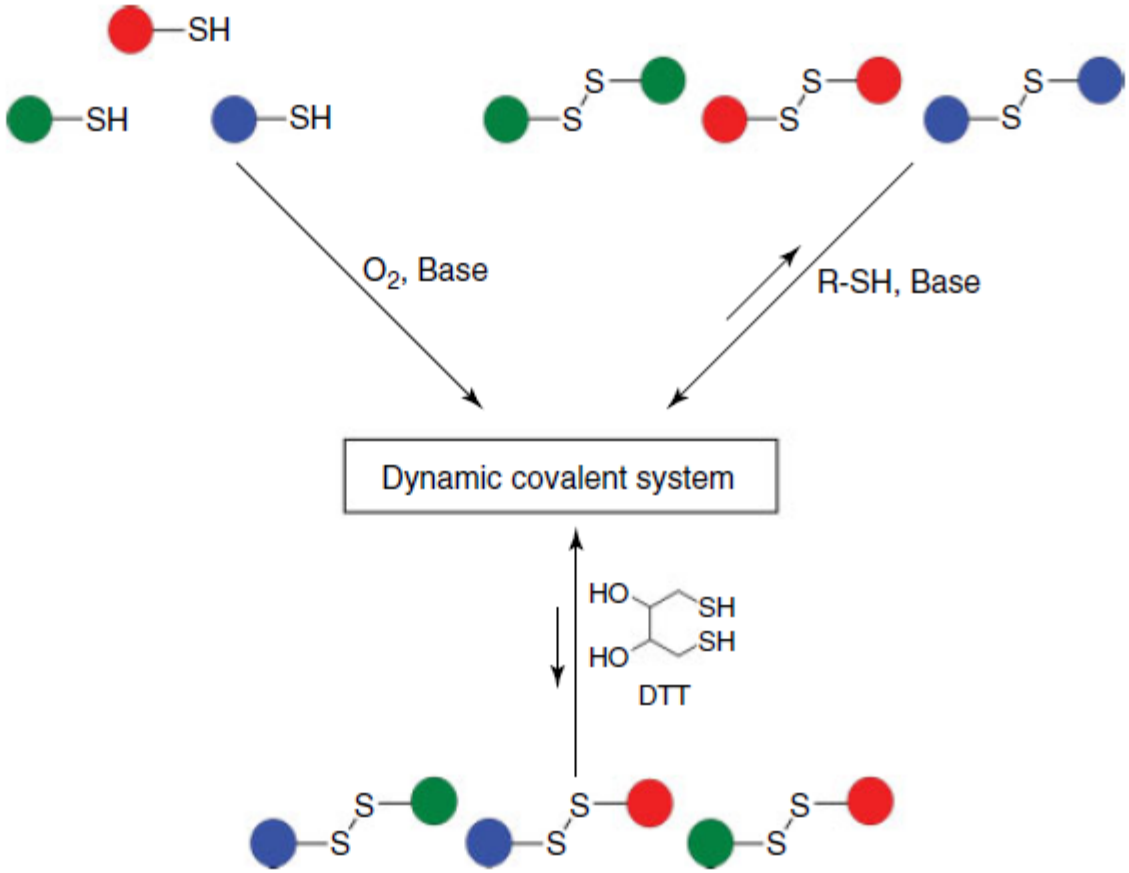

Figure 2 Possible pathways for the formation of a dynamic covalent system based on disulfide bonds.

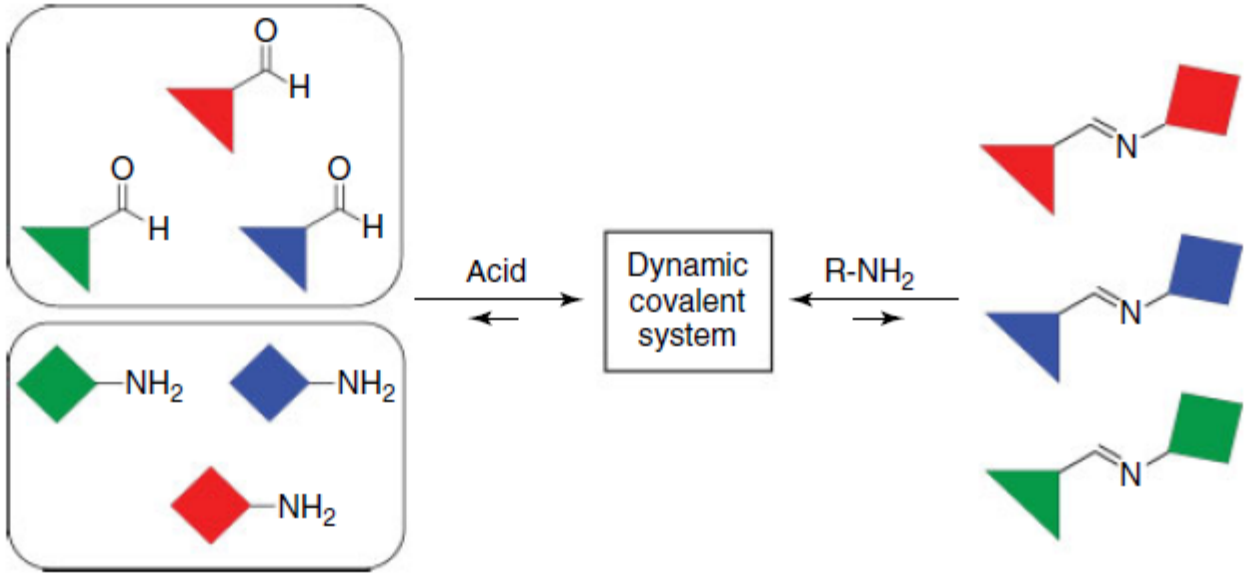

Figure 3 Possible pathways for the formation of a dynamic covalent system based on imine bonds.

VIP Supramolecular Chemistry

DOI: 10.1002/anie.200705272

Multicomponent Assembly of Boronic Acid Based Macrocycles and Cages**

*Nicolas Christinat, Rosario Scopelliti, and Kay Severin**

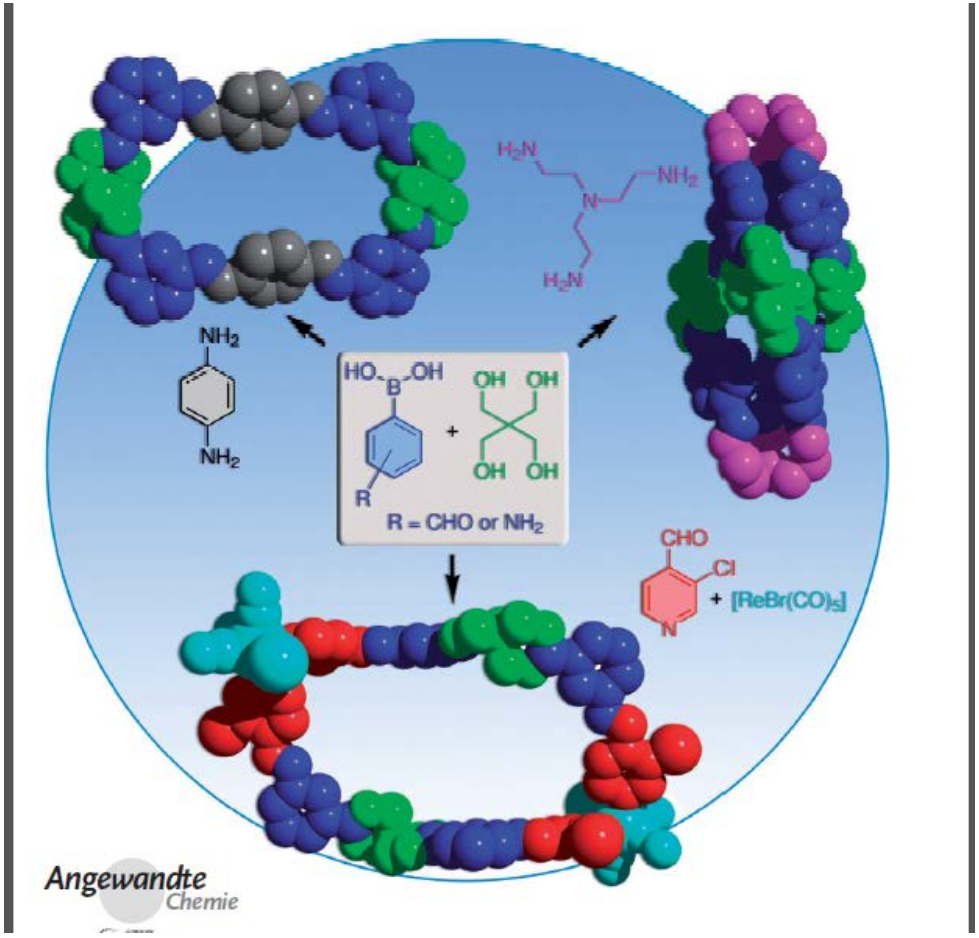

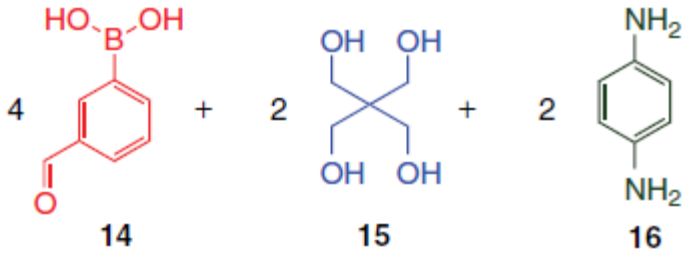

14 **15** **16**

$-12\ H_2O$ | $\xrightarrow[\text{THF/Toluene}]{\Delta}$

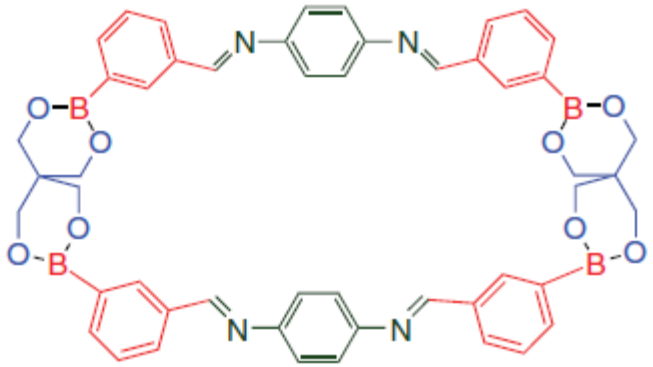

17

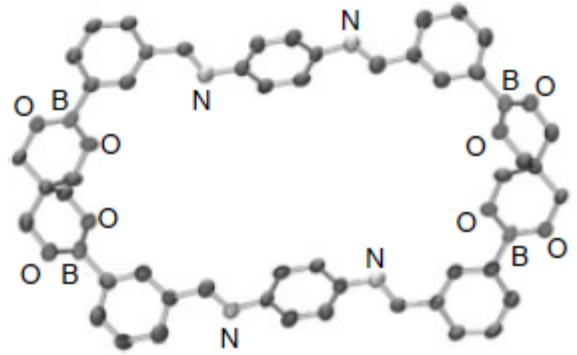

(a)

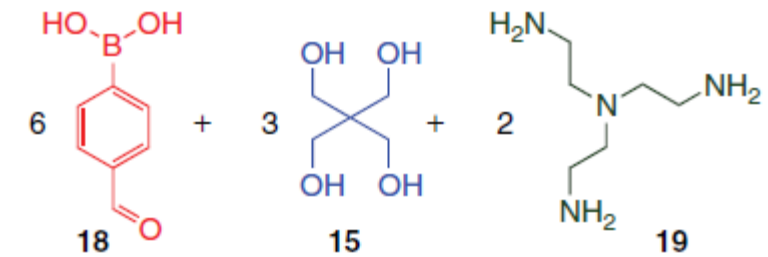
HO
B
OH
6
+
3
OH
OH
OH
OH
+
2
H_2N
N
NH_2
NH_2
18
15
19

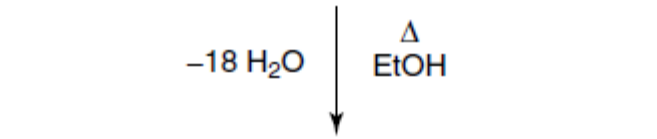
–18 H_2O
Δ
EtOH

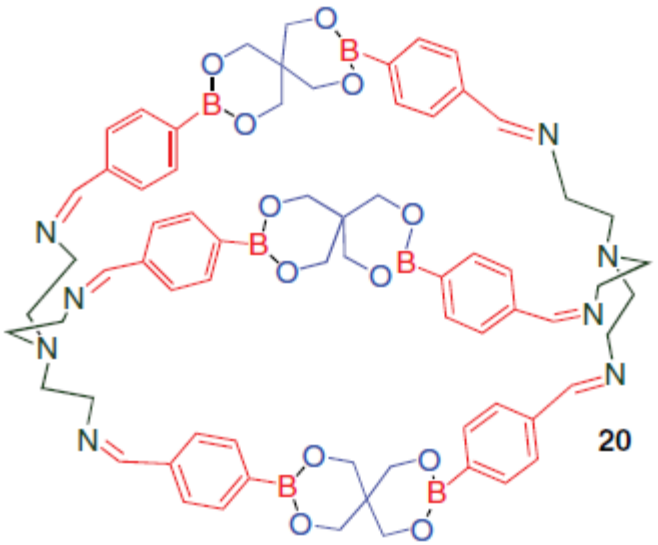
O
B
N
20

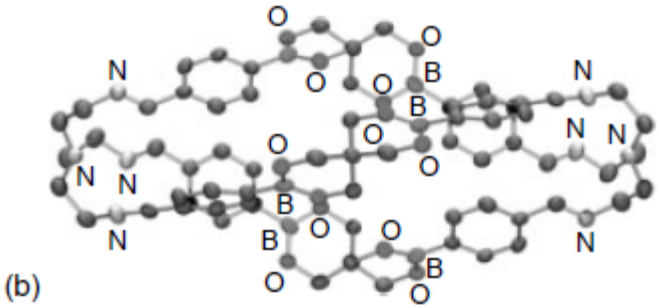
O
N
B
(b)